boundary. Examples given in Table I clearly show the efficiency of this method, with the residual error smaller than 100 ppm (0.01%), using only three to four modes in each region of the waveguide.

REFERENCES

[1] E. J. Rothwel and L. L. Frasch, "Propagation characteristics of dielectric-rod-loaded waveguides," *IEEE Trans. Microwave Theory Tech.,* vol. 36, pp. 594–600, Mar. 1988.

[2] S. P. Yeo, "Application of least–squares boundary residual method to the analysis of a circular waveguide loaded with nonconcentric dielectric rod," *IEEE Trans. Microwave Theory Tech.,* vol. 38, pp. 1092–1095, Aug. 1990.

[3] J. B. Davies and P. Nagenthiram, "Irregular fields, nonconvex shapes and the point-matching method for hollow waveguides," *Electron. Lett.,* vol. 7, pp. 401–404, July 1971.

[4] R. H. T. Bates, "General introduction to the extended boundary condition," in *Acoustic, Electromagnetic and Elastic Wave Scattering—Focus on the T-Matrix Approach*, V. K. Varadan and V. V. Varadan, Eds. New York: Pergamon, 1980, pp. 21–31.

[5] A. G. Ramm, "Justification of the T-matrix approach," in *Antennas Propagat. Int. Symp. Dig.,* Albuquerque, NM, 1982, pp. 13–14.

[6] ——, "Convergence of the T-matrix approach to scattering theory," *J. Math. Phys.,* vol. 23, no. 6, pp. 1123–1125, June 1982.

[7] D. Colton and R. Kress, "The unique solvability of the null field equations of acoustics," *Q. J. Mech. Appl. Math.,* vol. 36, pt. 1, pp. 87–95, Jan. 1983.

[8] P. Martin, "Acoustic scattering and radiation problems, and the null-field method," *Wave Motion,* pp. 391–408, Apr. 1982.

[9] J. R. Kuttler, "A new method for calculating TE and TM cutoff frequencies of uniform waveguides with lunar or eccentric annular cross section," *IEEE Trans. Microwave Theory Tech.,* vol. 32, pp. 348–353, Apr. 1984.

[10] M. Abramowitz and I. A. Stegun, *Handbook of Mathematical Functions.* New York: Dover, 1965.

3-D FEM/BEM—Hybrid Modeling of Surface Mounted Devices Within Planar Circuits

T. F. Eibert and V. Hansen

***Abstract*— Three–dimensional (3-D) finite-element (FE) meshes of surface-mounted devices (SMD's) are combined with the surface-current models of planar circuits in multilayered media. This is accomplished on the basis of Huygens' principle via the introduction of equivalent electric and magnetic surface-current densities on a surface enclosing the 3-D parts of the SMD's. The fields in the layered media are described by a surface integral equation based on the dyadic Green's function of the layered media. Special attention is directed to a proper interface of the surface and 3-D parts of the models. Numerical results for a homogeneous and a multilayered capacitor in a microstrip circuit are presented.**

***Index Terms*— Capacitors, finite-element methods, integral equations, nonhomogeneous media.**

Manuscript received October 29, 1997; revised April 3, 1998.

T. F. Eibert is with the Radiation Laboratory, Electrical Engineering and Computer Science Department, University of Michigan, Ann Arbor 48109-2122 USA

V. Hansen is with the Lehrstuhl für Theoretische Elektrotechnik, Bergische Universität/GH Wuppertal, 42119 Wuppertal, Germany.

Publisher Item Identifier S 0018-9480(98)06155-9.

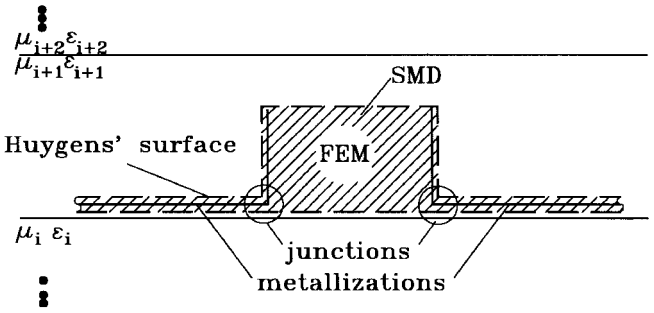

Fig. 1. Model of the field problem.

I. INTRODUCTION

Numerical modeling of circuits within multilayered media based on the analytic Green's-function description of the layered structure is usually restricted to the modeling of planar circuits or so-called two-and-one-half dimensional (2.5-D) circuits [1]. In [2] and [3], a hybrid method was presented, which combines the finite-element method (FEM) for the modeling of three-dimensional (3-D) inhomogeneities with a boundary-element method (BEM) for multilayered media. The investigated field problems where restricted to configurations where the 3-D finite-element (FE) models and surface-current models for metallic structures had no direct connection between each other. In this paper, it is illustrated how this method can be applied to modeling of surface-mounted devices (SMD's) within their planar-circuit environment. For this purpose, a connection between the surface-current models of the metallic parts of the circuits and the 3-D FE models of the SMD's is introduced. Numerical results for a homogeneous SMD capacitor and a multilayered SMD capacitor are shown.

II. FORMULATION

The model of the considered field problem is shown in Fig. 1. All disturbances of the multilayered structure are enclosed by a Huygens' surface. On the Huygens' surface, electric and magnetic surface-current densities are introduced according to

$$\vec{J}_A(\vec{r}) = \vec{n}(\vec{r}) \times \vec{H}(\vec{r}) \quad \vec{M}_A(\vec{r}) = -\vec{n}(\vec{r}) \times \vec{E}(\vec{r}). \tag{1}$$

This means that on metallizations, only electric surface-current densities are present. Further, the electric surface-current densities on the lower and upper parts of the Huygens' surface at the metallizations can be added for metallizations with vanishing thickness and be interpreted as the physical electric surface-current density within the metallization.

The fields of the Huygens' current densities within the multilayered medium are described with a surface integral representation, whereas the fields in the SMD are modeled by the FEM. The connection between the two different field formulations are given by the boundary conditions for the tangential-field components on the Huygens' surface. Further details of the basic formulation of the method can be found in [2] and [3].

For the discretization of the model, care must be taken so that Kirchhoff's current-continuity formula is satisfied at the junctions between the metallizations and SMD. In typical edge-based discretization meshes, this is a problem because only one edge is generated at the junctions where three triangles meet. That is, only one independent current will be present at the junction if one unknown

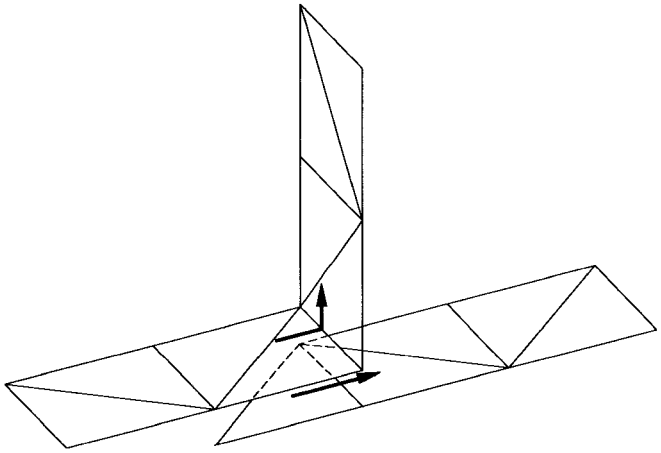

Fig. 2. Modeling of Huygens' surface junctions.

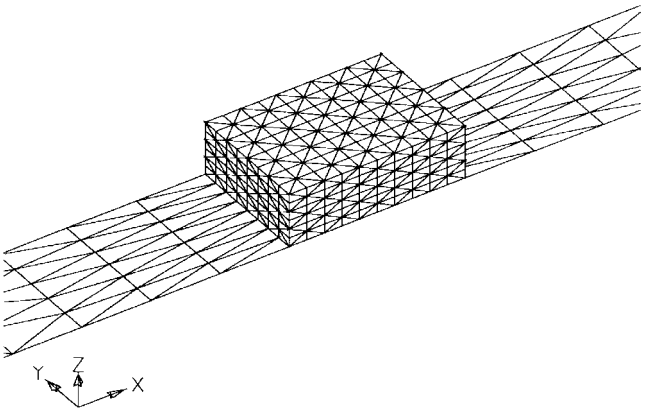

Fig. 3. Mesh for homogeneous capacitor, 2400 tetrahedra, $\varepsilon_r = 100$.

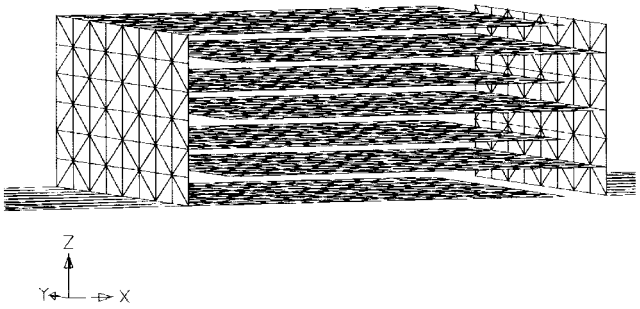

Fig. 4. Mesh for multilayered capacitor, 2400 tetrahedra, $\varepsilon_r = 6$.

is generated per edge. To overcome this, the mesh at the junctions is modified, as illustrated in Fig. 2. One of the three triangles is doubled so that two identical triangles at the same position result (drawn with finite distance in the figure). Each of the two identical triangles is connected to one of the remaining triangles at the junction giving rise to two independent currents across the junction. For each of these currents, one edge connecting two triangles is present, which allows the use of the original edge-based code without further changes and without violating Kirchhoff's current-continuity formula.

III. Applications and Results

A homogeneous SMD capacitor and a multilayered capacitor were investigated with the described method. The discretization models are shown in Figs. 3 and 4. For the multilayered capacitor, the volume elements are omitted, and only the discretization of the

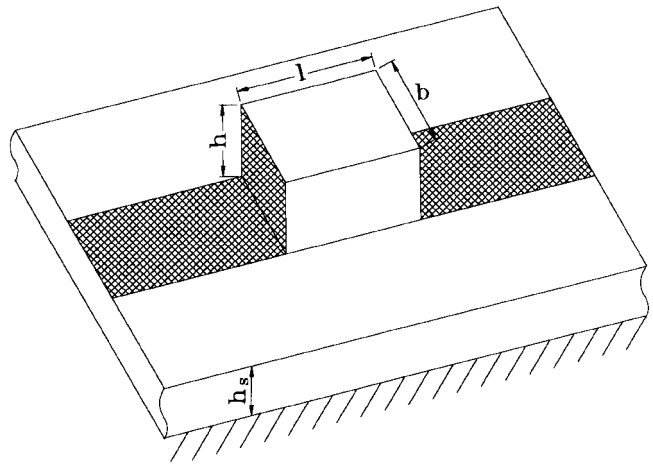

Fig. 5. Circuit configuration, $h_s = 0.8$ mm, $l = 3.2$ mm, $b = 2.25$ mm, $h = 1.3$ mm, $\varepsilon_{r,s} = 2.54$.

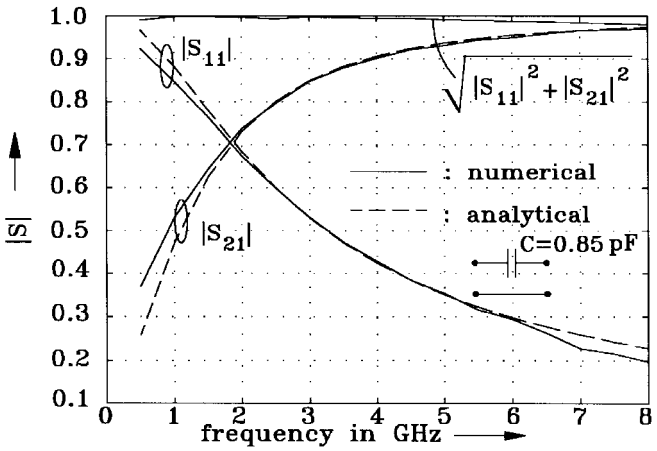

Fig. 6. S-parameters for homogeneous capacitor.

metallization planes is shown. The metallization of the homogeneous capacitor is restricted to the side faces connected to the microstrip line. The circuit configuration and associated dimensions (equal for the two discretization models) are given in Fig. 5. Corresponding S-parameter calculations are illustrated in Figs. 6 and 7, and were derived from the current distributions on the microstrip-line portions of the discretization models after extracting the line propagation constants using Prony's method. The S-parameters of the homogeneous capacitor are compared to analytic results of a 0.85-pF lumped capacitor. It can be seen that the effective capacitance of the SMD capacitor within the microstrip line is even larger than this value in the lower frequency range (estimation with parallel-plate model is approximately 0.82 pF), whereas the effective capacitance decreases for higher frequencies. The results for the multilayered capacitor are compared to a 10-pF lumped capacitor. It is important to recognize that a very strong resonance is present at about 4.35 GHz, whereas in the case of the homogeneous capacitor, no resonances are observed. Further calculations with the multilayered capacitor showed that for smaller capacitance values, the resonance shifts to larger frequencies according to $f_{\rm res} = 1/\sqrt{LC}$ where the parasitic inductance L of the capacitor is constant.

IV. Conclusion

A full-wave 3-D modeling of SMD's within their planar-circuit environment was performed using a FEM/BEM hybrid approach.

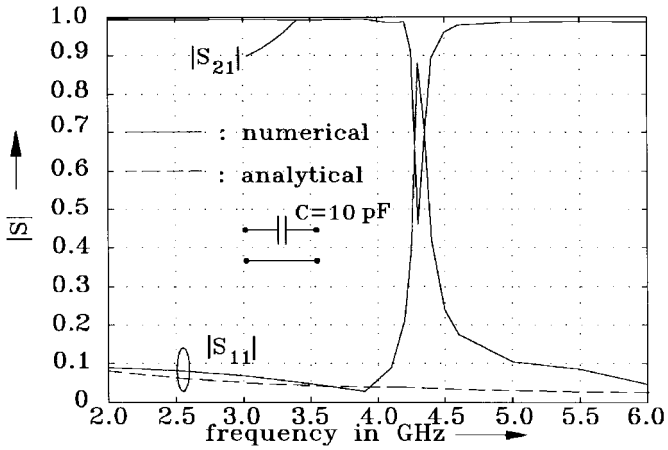

Fig. 7. S-parameters for multilayered capacitor.

An important part of the modeling procedure was the interface of the 3-D model for the SMD's with the surface-current model of the metallizations forming the planar circuit. Using this method, we investigated homogeneous and multilayered SMD capacitors within a microstrip circuit. For the homogeneous capacitor, we could not observe any resonances, although the shortest wavelength in the dielectric was shorter than the length of the capacitor. For the multilayered capacitor with larger capacitances, we found resonances with frequencies dependent on the capacitance values.

REFERENCES

[1] M.-J. Tsai, C. Chen, N. G. Alexopoulos, and T.-S. Horng, "Multiple arbitrary shape via-hole and air-bridge transitions in multilayered structures," *IEEE Trans. Microwave Theory Tech.*, vol. 44, pp. 2504–2511, Dec. 1996.

[2] T. F. Eibert and V. Hansen, "3D FEM/BEM—Hybrid approach for planar layered media," *Electromagn.*, vol. 16, no. 3, pp. 253–272, May/June 1996.

[3] ——, "3-D FEM/BEM—Hybrid approach based on a general formulation of Huygens' principle for planar layered media," *IEEE Trans. Microwave Theory Tech.*, vol. 45, pp. 1105–1112, July 1997.

TM Scattering from Hollow and Dielectric-Filled Semielliptic Channels with Arbitrary Eccentricity in a Perfectly Conducting Plane

W. J. Byun, J. W. Yu, and N. H. Myung

***Abstract*— The behavior of TM wave scattering from hollow and dielectric-filled semielliptic channels in a perfectly conducting substrate is investigated. The scattered field is represented in terms of an infinite series of Mathieu functions with unknown coefficients. By applying the separation of variables and employing the partial orthogonality of the first-kind angular Mathieu functions, the unknown coefficients are obtained. Numerical results are given for the scattered-field patterns by the channels with different eccentricities and permittivities.**

***Index Terms*—Electromagnetic scattering, Mathieu functions, semielliptic channel.**

I. INTRODUCTION

A considerable number of investigations have been performed on the radar cross section (RCS) analysis for the geometries with channels, grooves, and cracks in a perfectly electric conducting (PEC) substrate. This is due to the fact that these local guiding structures may excite internal resonances, and they sometimes yield scattering contribution which cannot be obtained with other ordinary geometries. The electromagnetic scattering effect from a square groove in a PEC substrate has been treated in [1] and a semicircular one treated in [2]–[4]. However, a scattering solution is not available for semielliptic channels in a PEC substrate. In this paper, TM scattering from semielliptic channels is solved with different eccentricities and permittivities in a PEC plane by employing the separation of variables and mode-matching method. In elliptic cylinder coordinates, separation of variables leads to Mathieu's equation, which has solutions in the form of Mathieu functions [5]. Although the familiar orthogonality relationships at the interface cannot be applied for the scattering problem of dielectric-filled geometries, an analytic-series solution to electromagnetic scattering by dielectric-filled semielliptic channels is presented in this paper.

II. FIELD REPRESENTATIONS

The problem is formulated with respect to elliptic cylinder coordinates ζ and η where $x = d, \cosh\zeta, \cos\eta$, $y = d, \sinh\zeta, \sin\eta$, and d is the semifocal distance in Fig. 1. The semielliptic interface between Regions I and II is represented by the relation ζ_0 $(e = 1/\cosh\zeta_0 = d/a)$. The eccentricity e is represented by $\sqrt{1-(b/a)^2}$, and a and b are semimajor and semiminor axis, respectively. The normalization factors adopted by Ince [6] are used, and Mathieu functions are computed using the algorithms in [7]. Throughout this paper, the $e^{j\omega t}$ time–harmonic factor is assumed and suppressed. The TM_z plane wave impinges on a dielectric-filled semielliptic channel in a PEC substrate at the incident angle of ϕ_i with respect to the x-axis, as shown in Fig. 1. The semielliptic channel has a wavenumber $k_1 (= \omega\sqrt{\mu_0\epsilon_0\epsilon_r})$. When the incident wave impinges on the channel in a PEC substrate, a surface scattering

Manuscript received August 1, 1997; revised January 26, 1998.

The authors are with the Department of Electrical Engineering, Korea Advanced Institute of Science and Technology (KAIST), Taejon 305-701, Korea (e-mail: nhmyung@eekaist.kaist.ac.kr; bwj@cais.kaist.ac.kr).

Publisher Item Identifier S 0018-9480(98)06156-0.